

**Supporting Information**

**Stalagmite-like Self-cleaning Surfaces Prepared by Silanization of Plasma-  
induced Metal-oxide Nanostructures**

*Ching-Yu Yang<sup>1,2</sup>, Shang-I Chuang<sup>1</sup>, Yu-Hsiang Lo<sup>1</sup>, Hsin-Ming Cheng<sup>\*2</sup>, Jenq-Gong Duh<sup>1</sup>, Po-Yu  
Chen<sup>1\*</sup>*

*<sup>1</sup>Department of Materials Science and Engineering, National Tsing Hua University, Hsinchu 101,  
Sec. 2, Kuang-Fu Rd., Hsinchu 30013, Taiwan*

*<sup>2</sup>Material and Chemical Research Laboratories, Industrial Technology Research Institute, 195, Sec.  
4, Chung Hsing Rd., Chutung, Hsinchu 31040, Taiwan*

**\*Corresponding authors: SMCheng@itri.org.tw, poyuchen@mx.nthu.edu.tw**

**Tables:****Table S1.** Measurements of SCA, CAH and sliding angle toward water, glycerol and n-Hexadecane on SCWO coatings fabricated by 20-sec deposition duration under the APP system.

Number	Liquid	Surface Tension (dyn/cm)	SCA (°) <sup>a)</sup>	CAH ( $\theta_{adv}/\theta_{red}$ )(°)	Sliding Angle (°)
1	DI water	72.8	162.9 ± 2.6	2 (161/159)	1
2	Glycerol	64	162.1 ± 0.9	17 (160/144)	1.8
3	Ethylene Glycol	47.3	148.5 ± 2.2	21 (154/133)	> 40
4	n-Hexadecane	27.5	130.3 ± 0.4	99 (129/ 30)	--

<sup>a)</sup> Due to the superior anti-wettability of the synthesized SCWO coating, the liquid drops of water and glycerol could not attach on the surface even when the liquid volume was increased to ~ 10  $\mu$ L. Hence, the SCA of water and glycerol were measured from the pendant drops which was just contact the surface of the substrate (i.e. the dispense tip was still in the drop).

**Table S 2.** Comparison of the experimental contact time of a water bouncing drop for the present work and past studies.

<b>Reference</b>	<b>Year</b>	<b>Radius of droplet (mm)</b>	<b>Total contact time (ms)</b>	<b>Dimensionless time (<math>t_c^*</math>)</b>
Ref. [1] <sup>1</sup>	2008	1	16	4
Ref. [2] <sup>2</sup>	2008	1.35	23	4
Ref. [3] <sup>3</sup>	2009	1	12.5	3
Ref. [4] <sup>4</sup>	2010	1.5	20	2.9
Ref. [5] <sup>5</sup>	2012	0.022	0.032	2.6
Ref. [6] <sup>6</sup>	2013	1.3	7.8	2.2
<b>Present work</b>	<b>2015</b>	<b>1.2</b>	<b>9.76</b>	<b>2</b>

**Table S 3.** Summary of the position, height, corresponding time, calculated potential energy and energy dissipation for each half cycle comparing to the original position of water droplet on SCWO-coated PET film.

Number	Position-X (mm) <sup>a)</sup>	Height-Y (mm)	Time (ms)	Potential Energy (Joules) <sup>b)</sup>	Energy Dissipation (%) <sup>c)</sup>
1	10.2	6	0	$4.6 \times 10^{-7}$	--
2	-8.5	4.8	160.5	$3.7 \times 10^{-7}$	-19.3
3	7.8	4.6	266.5	$3.5 \times 10^{-7}$	-5.4
4	-6.5	3.7	374.5	$2.8 \times 10^{-7}$	-18.4
5	6.1	3.3	480.5	$2.5 \times 10^{-7}$	-11.3
6	-4.9	2.6	570.5	$2.0 \times 10^{-7}$	-20.6
7	4.1	2.3	665.0	$1.7 \times 10^{-7}$	-14.0
8	-2.4	1.5	762.0	$1.1 \times 10^{-7}$	-34.9
9	1.8	1.4	852.0	$1.0 \times 10^{-7}$	-7.1
10	-0.8	1.2	926.5	$8.8 \times 10^{-8}$	-15.4
11	0.5	1.1	1039.0	$8.2 \times 10^{-8}$	-6.8

<sup>a)</sup> By setting the lowest point of U-shape PET film as the origin of coordinate, the Position-X is the projection of the water droplet on the X coordinate; <sup>b)</sup> The potential energy was calculated as  $U = mgh$ , where  $m$  is the mass of droplet ( $\sim 7.8 \times 10^{-6}$  g for  $7.7 \mu\text{L}$  of water).  $g$  is the acceleration of gravity.  $h$  is defined as the height measured from the trajectory of water droplet; <sup>c)</sup> The calculated energy dissipation of each half cycle, in average, was 15.32%, and the standard deviation was 8.76%.

**Table S 4.** The testing conditions for sand abrasion and the corresponding sliding angles for the tested samples.

<b>Number</b>	<b>Impinged height (cm)</b>	<b>Test duration (s)</b>	<b>SCA (°)</b>	<b>Sliding angle (°)</b>
1	30	30	160.0 ± 2.0	< 5
2	30	50	145.7 ± 1.8	> 45
3	60	30	148.5 ± 2.0	> 45
4	60	50	137.9 ± 1.5	Droplet pinning
5	60	100	130.1 ± 2.1	Droplet pinning

Figures:

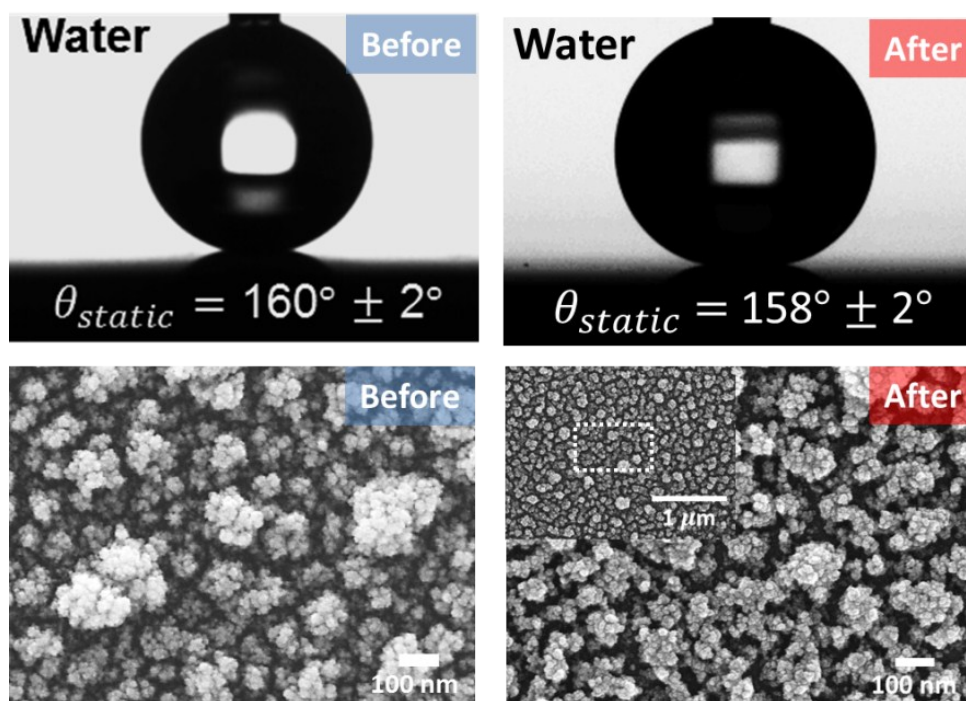


**Fig. S 1** The contact angle measurement of the SCWO-coated silicon substrates before and after the water stream test.

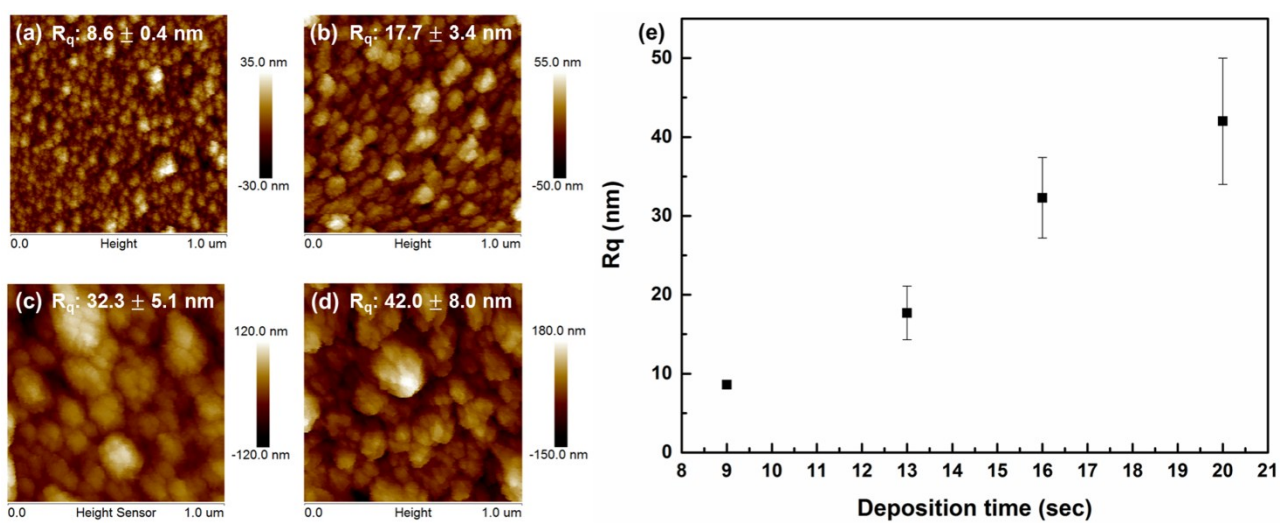


**Fig. S 2.** AFM images of the stalagmite-like protrusions fabricated under the APP system for (a) 9 sec, (b) 13 sec, (c) 16 sec, (d) 20 sec. All the samples were modified with FAS after APP treatment. (e) The corresponding values of  $R_q$  characterized by AFM.

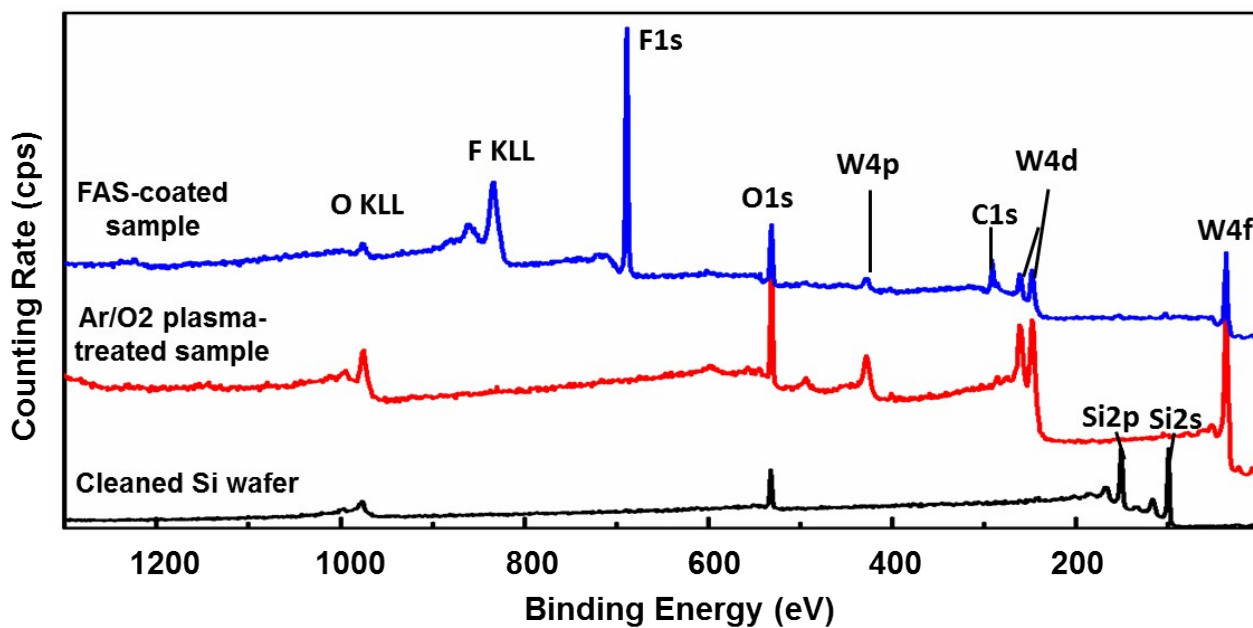
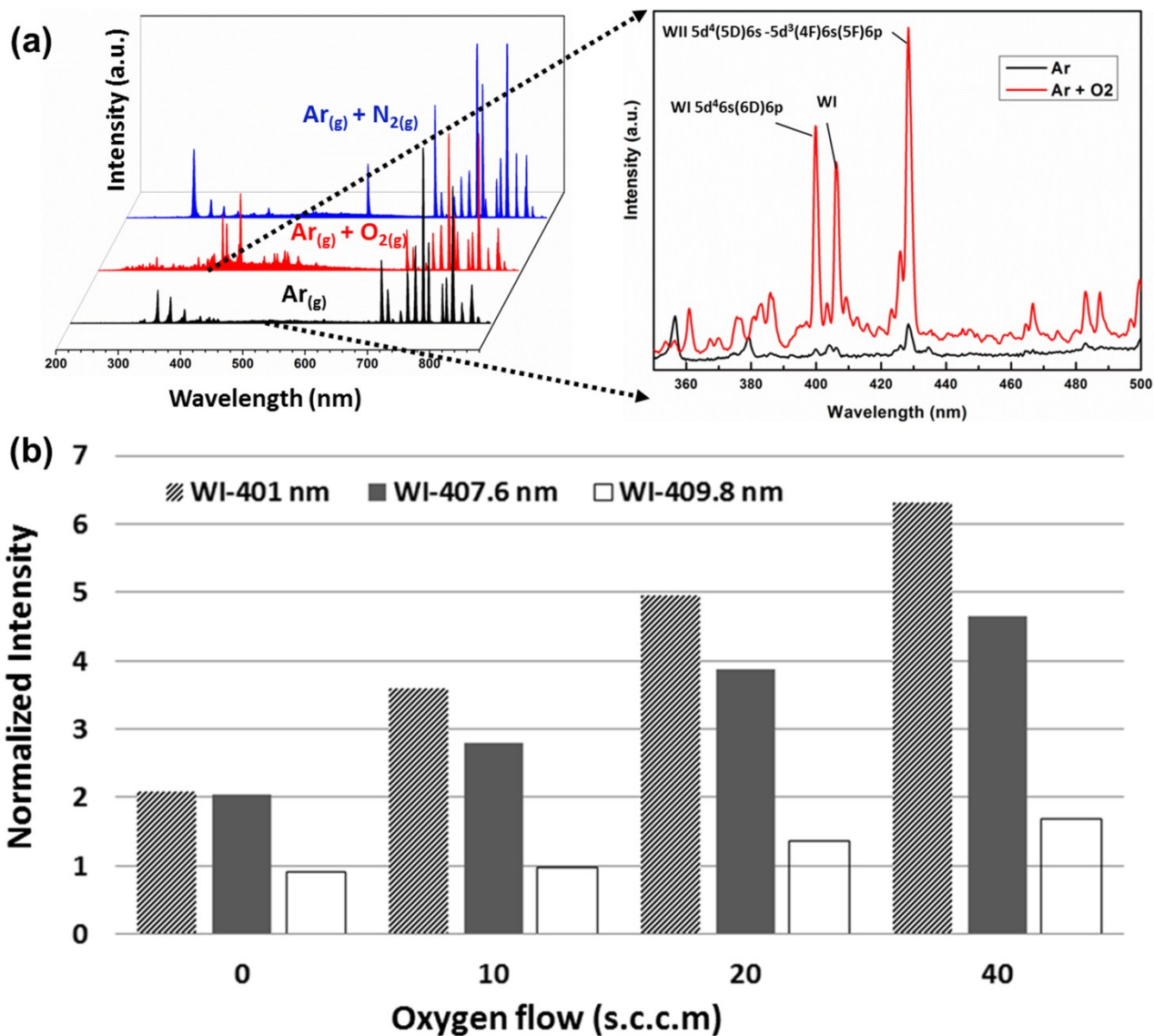
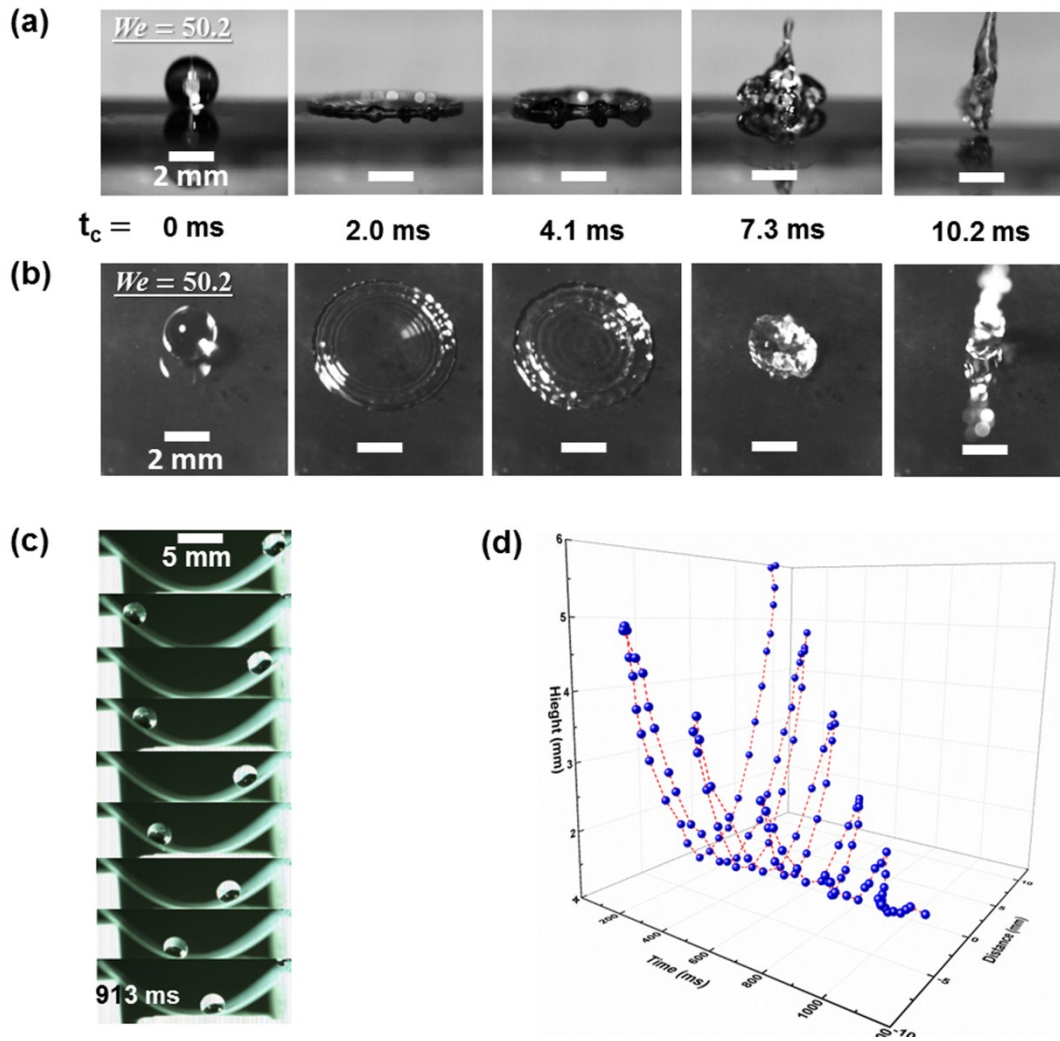


Fig. S 3. XPS spectra for the FAS-coated, Ar/O<sub>2</sub> plasma treated and well-cleaned samples.



**Fig. S 4.** (a) Optical electron spectra for three different reaction atmospheres (Ar, Ar+O<sub>2</sub> and Ar+N<sub>2</sub>). Most the characteristics peaks of excited argon ions were detected within 700 to 850 nm. The peaks observed within 400 to 500 nm were mainly detected from the tungsten ions. (b) The three characteristic peaks corresponding to the tungsten atomic lines exhibited higher normalized intensity with increasing the oxygen flow, indicating that the formation of tungsten and tungsten oxide film was contributed by the frequent collision between oxygen radicals and tungsten electrode of atmospheric pressure plasma system.



**Fig. S 5.** Impact dynamics and the trajectory of a water droplet on the SCWO-coated samples: (a) The side-view of selected high-speed images of the bouncing drop detached from the coated silicon surface after 10.2 ms. (b) The top-view images show that the water drop bounced off the surface with axial symmetry. (c) A series of images of water droplet rolling and (d) the corresponding trace which was calculated from the high-speed images on the curved PET film.

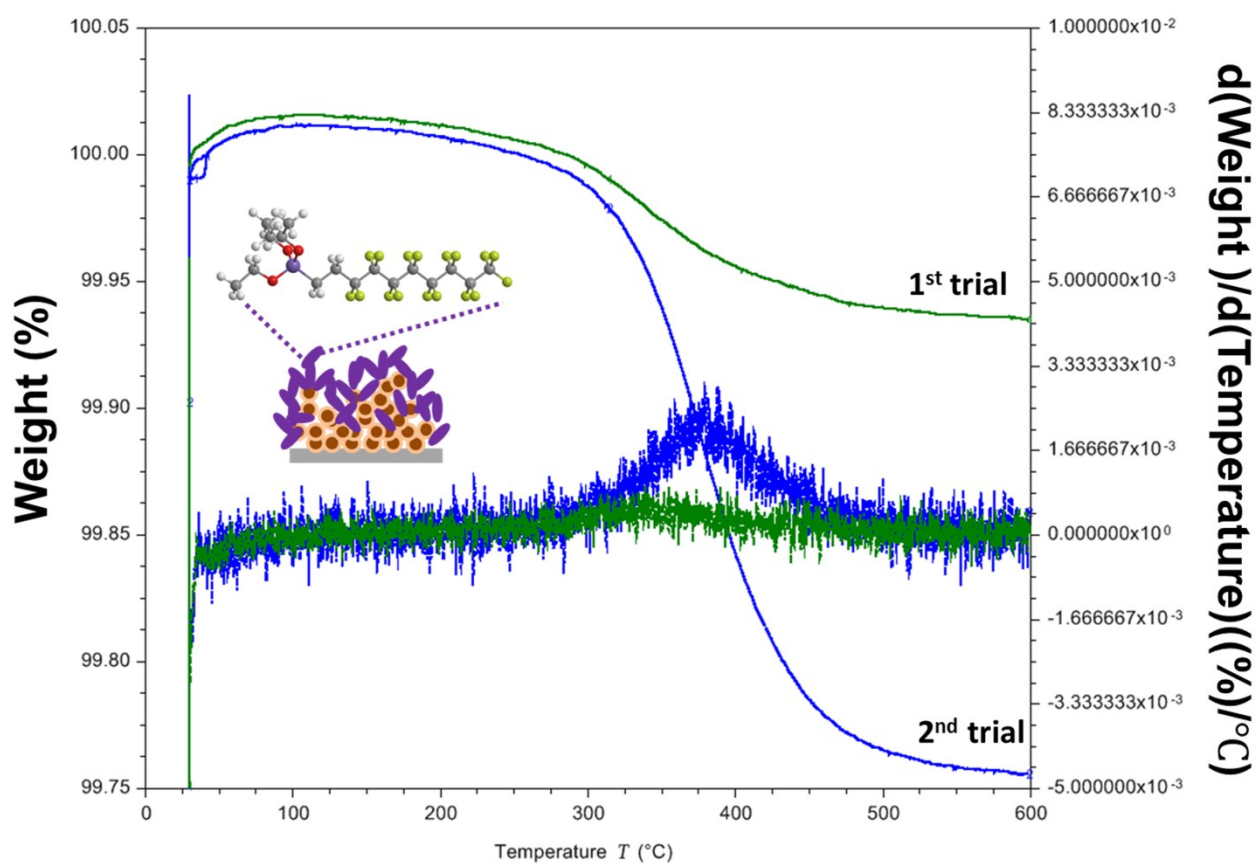


**Fig. S 6.** Thermogravimetric analysis (TGA) of the SCWO-coated silicon wafer revealed that the major weight loss occurred within the range of 330°C to 380°C under oxygen atmosphere.

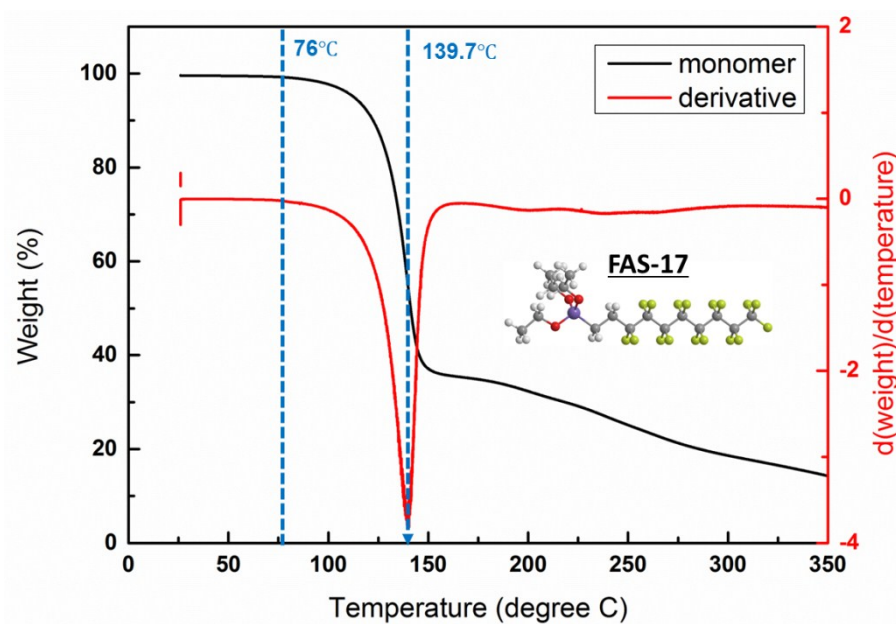


**Fig. S 7.** Thermogravimetric analysis (TGA) of FAS-17 indicated that the initial weight loss occurred at 76°C and the weight underwent obviously drop at 139.7°C.

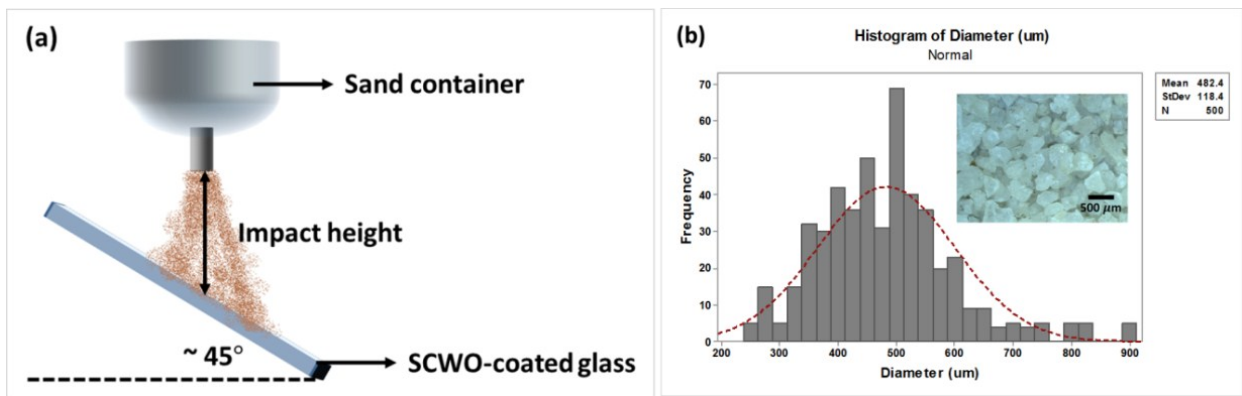


**Fig. S 8.** (a) Sand abrasion test and (b) the particle size distribution of sand grains.

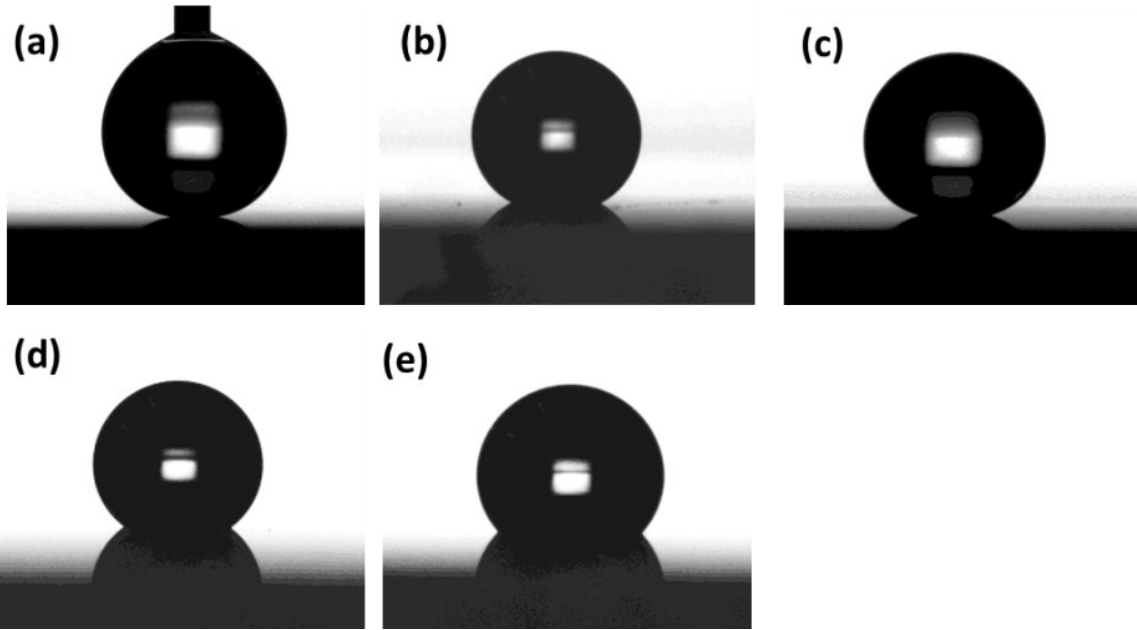


**Fig. S 9.** The corresponding contact angles measured from the samples after the sand abrasion under different testing conditions. (a) Impact height: 30 cm, test duration: 30 sec, SCA:  $160^{\circ} \pm 2^{\circ}$ ; (b) Impact height: 30 cm, test duration: 50 sec, SCA:  $145.7^{\circ} \pm 1.8^{\circ}$ ; (c) Impact height: 60 cm, test duration: 30 sec, SCA:  $148.5^{\circ} \pm 2^{\circ}$ ; (d) Impact height: 60 cm, test duration: 100 sec, SCA:  $130.1^{\circ} \pm 2.1^{\circ}$ .

## Videos:

- **Video S1:** Demonstration of the liquid-repellency toward glycerol.
- **Video S2:** Demonstration of the transparent self-cleaning SCWO coating on glass substrate.
- **Video S3:** Sand abrasion test on SCWO-coated glass. The impact height is 30 cm, and the weight of sand is 30 g.

The sand abrasion test which we conducted on SCWO-coated glass simulating the dynamic wears resulted by aerosol particles in outdoor environment, (Fig. S8a). The SCWO-coated glass was attached on a 45-degree slope<sup>7</sup>. The sand was composed of silica, which was purchased from a local vendor in Taiwan. The average grain size was  $482.4 \text{ nm} \pm 118.4 \text{ nm}$  measured from 500 sand grains under optical microscope (Fig. S8b). Different quantities of sand (30 g, 50 g, and 100 g) were poured in the sand container, respectively, and impinged the SCWO-coated glass from heights of 30 cm and 60 cm (Table S4). The sand consuming rate was controlled at approximately 1 g/s and the impact energy of a sand grain was calculated as follows:

$$E_{\text{impact}} = m_s gh = 4/3\pi\rho R_s^3 gh$$

where  $\rho$  is the density of silica ( $\sim 2 \text{ g/cm}^3$ ).  $g$  is the acceleration of gravity.  $R_s$  represents the radius of sand grain ( $\sim 240 \text{ }\mu\text{m}$ ), and  $h$  is defined as the impact height. The corresponding energies of a sand grain impinging the surface of SCWO from 30 and 60 cm were determined to be  $3.3 \times 10^{-7} \text{ J}$  and  $6.7 \times 10^{-7} \text{ J}$ , respectively.

The corresponding contact angles after sand abrasion tests were measured, as shown in Fig. S9. When the total sand weight was controlled under 30 g, the SCWO-coated glass remained good superhydrophobicity and showed the sliding angle less than  $5^\circ$  toward water after sand impingement from 30 cm. The stalagmite-like protrusions modified with multilayer FAS molecules sustained the sand abrasion. According to the literature<sup>8</sup>, outdoor aerosol particles exhibited a wide range of diameters, ranging from nanometers to micrometers, whereas they hardly exceeded  $10 \text{ }\mu\text{m}$ . Therefore, we selected  $R_A = 10 \text{ }\mu\text{m}$  as the reference diameter for calculating the corresponding velocity<sup>9</sup> for aerosol particles under the lower limit of impact energy ( $E_{\text{impact}} = 3.3 \times 10^{-7} \text{ J}$ ) as follows:

$$E_{\text{impact}} = 1/2 m_A V_A^2$$
$$V_A = \sqrt{\left[ \frac{(2 \times E_{\text{impact}})}{m_A} \right]} = \sqrt{\left[ \frac{2 \times E_{\text{impact}}}{\left( \frac{4}{3} \pi R_A^3 \times \rho \right)} \right]} \cong 250 \text{ km/h}$$

According to the sand abrasion results, we demonstrated that the SCWO coatings could be

suitable for superhydrophobic applications in both outdoor and indoor environment.

- **Video S4:** After 30 g-sand-abrasion testing, SCWO-coated glass can still perform superior water-repellency and low sliding angle  $< 5^\circ$ .

## References

1. Y. C. Jung and B. Bhushan, *Langmuir*, 2008, **24**, 6262-6269.
2. P. Brunet, F. Lapierre, V. Thomy, Y. Coffinier and R. Boukherroub, *Langmuir*, 2008, **24**, 11203-11208.
3. P. Tsai, S. Pacheco, C. Pirat, L. Lefferts and D. Lohse, *Langmuir*, 2009, **25**, 12293-12298.
4. L. Mishchenko, B. Hatton, V. Bahadur, J. A. Taylor, T. Krupenkin and J. Aizenberg, *ACS Nano*, 2010, **4**, 7699-7707.
5. D. Hee Kwon and S. Joon Lee, *Appl. Phys. Lett.*, 2012, **100**, 171601.
6. J. C. Bird, R. Dhiman, H.-M. Kwon and K. K. Varanasi, *Nature*, 2013, **503**, 385-388.
7. X. Deng, L. Mammen, H.-J. Butt and D. Vollmer, *Science*, 2012, **335**, 67-70.
8. J. Heintzenberg, F. Raes and S. E. Schwartz, *In Atmospheric Chemistry in a Changing World*, Springer, Berlin, 2003.
9. X. Deng, L. Mammen, Y. Zhao, P. Lellig, K. Müllen, C. Li, H.-J. Butt and D. Vollmer, *Adv. Mater.*, 2011, **23**, 2962-2965.